Vanadyl(IV) porphyrin dimers with palladium(II) and platinum(II) linkages: syntheses, electronic properties and magnetic interactions between the two moieties

Jordan L Appleton, Nolwenn Le Breton, Mary-Ambre Carvalho, Jean Weiss, Athanassios K Boudalis, Christophe Gourlaouen, Sylvie Choua, Romain Ruppert

Vanadyl(IV) porphyrin dimers with palladium(II) and platinum(II) linkages: syntheses, electronic properties and magnetic interactions between the two moieties

Jordan L. Appleton, Nolwenn Le Breton, Mary-Ambre Carvalho, Jean Weiss, Athanassios K. Boudalis, Christophe Gourlaouen, Sylvie Choua and Romain Ruppert*

Institut de Chimie, UMR CNRS 7177, Universite de Strasbourg, 4 rue Blaise Pascal, 67000 Strasbourg (France).

Porphyrinoids, vanadylporphyrin, EPR, magnetic interaction, porphyrin dimer.

ABSTRACT: We report the synthesis of new vanadylporphyrins bearing peripheral coordination sites. By using palladium(II) or platinum(II) as connecting ions, porphyrin dimers were isolated and characterized by X-ray crystallography. These paramagnetic species were studied by electronic spectroscopy and Continuous Wave Electron Paramagnetic Resonance (CW EPR). Large bathochromic shifts were observed by comparing porphyrin monomers and dimers showing that electronic delocalization was present as demonstrated earlier for diamagnetic compounds. Despite the large distance (> 14 Å) between the two vanadyl centers in these dimers, small dipolar interactions between the two paramagnetic ions could be determined.

INTRODUCTION

Magnetic interactions between distant metal ions has been a main research area in molecular magnetism for many years.[1] Recently transition metal complexes became the subject of studies leading to potential applications in quantum information processing (QIP).[2] Among metal ions vanadium(IV) seems to fulfil many pre-requisites for QIP applications: (i) well-known chemistry to design and prepare new complexes, (ii) long coherence times and (iii) convenient hyperfine coupling[3] permitting its additional use as a spin qubit with its high-dimensional Hilbert space.[4] Several different vanadium(IV) complexes, mainly vanadyl, $[VO]^{2+}$, complexes have been reported, prepared and studied using EPR spectroscopy. Most of the vanadium(IV) complexes studied were mononuclear.[5] In the last years several dinuclear vanadyl(IV) complexes were proposed for potential two qubits systems. One of the main objectives of this coordination chemistry approach is the design and preparation of molecules with two spins localized in a rigid and preferably planar scaffold, controlling precisely the distance between the two metal centers.[6-12] Among potential candidates for vanadyl(IV) complexes, the porphyrin ligand seems to be a good candidate as a starting building block.[13] Vanadyl(IV) porphyrins are extremely stable compounds, as demonstrated by their presence in oil samples as thermodynamic end products resulting from the degradation of all tetrapyrrolic pigments of life.[14] The functionalization of the porphyrin periphery (or other porphyrinoids) is also well developed and many examples of porphyrinoid dimers were described in the literature.[15-21] It was demonstrated quite early that in the fused porphyrinic dimers described by the group of Osuka, the antiferromagnetic couplings between copper(II) or silver(II) diporphyrins were strongly dependent on the type of connections.[22] Very recently, the group of Anderson proposed vanadyl(IV) porphyrin dimers as quantum mediators for vanadyl qubits.[23] Our group has shown earlier that porphyrins bearing additional external coordination sites can be used to construct dimers or oligomers by linking these building blocks with different metal ions (see Chart 1).[24-27]

Chart 1. Molecular formula of porphyrin dimers linked by metal ions (M_1, M_3 = Ni(II), Zn(II), H_2, Cu(II), Pd(II), M_2 = Ni(II), Cu(II), Pd(II), Pt(II)).

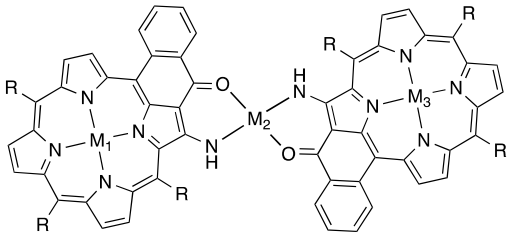

Extended electronic delocalization was present in these large molecules. Strong antiferromagnetic coupling was found for copper(II) porphyrins linked by copper(II) or and a small coupling was found for copper(II) porphyrins linked by palladium(II) ions.[28] We describe here the syntheses of vanadyl(IV) porphyrin monomers and palladium(II) or platinum(II) linked vanadyl(IV) porphyrin dimers, their structural characterizations, and the study of these new molecules by Electron Paramagnetic Resonance (EPR).

RESULTS AND DISCUSSIONS

The starting porphyrin bases **1** and **2** were prepared by following procedures developed earlier in our group.[29] Metalation of the ketoporphyrins with vanadium(IV) sulfate was almost quantitative and afforded vanadylporphyrins **3** and **4**.[30] The known amination of these ketoporphyrins was realized with the Katritzky reagent and gave the desired vanadylenaminoporphyrins **5** and **6** in good yields. Compounds **5** and **6** differ mainly by their solubility properties and the steric hindrance near the external coordination site.

Scheme 1. Preparation of the vanadylporphyrins.

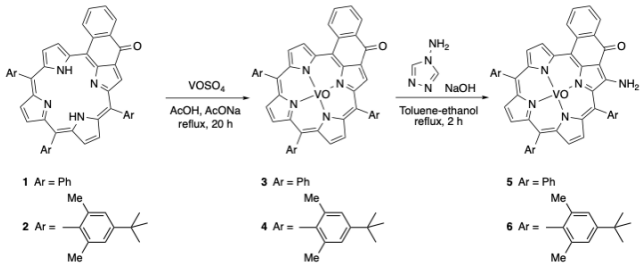

With *meso*-phenyl groups, single crystals could be grown from chloroform/methanol and the X-ray structure solved. Vanadyl(IV)porphyrins found in the CCDC crystallographic base present a square pyramidal coordination geometry with the vanadium(IV) located outside the plane of the aromatic macrocycle.

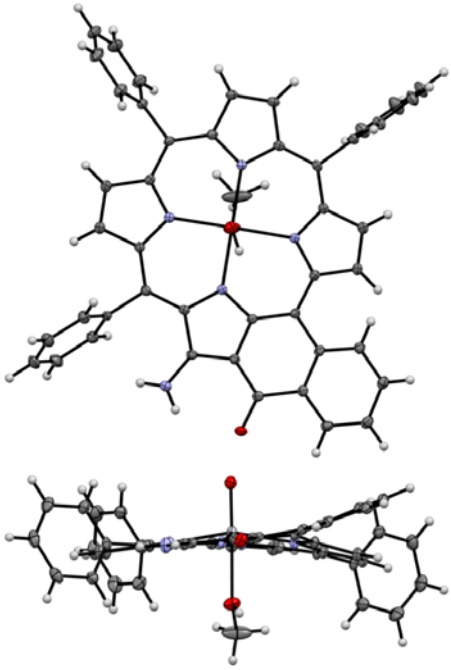

Figure 1. X-ray structure of starting vanadylporphyrin 5: two orthogonal views showing the distorted aromatic macrocycle and the unusual coordination geometry around the vanadium(IV) ion.

Surprisingly, for compound **5**, the coordination geometry is different and the vanadium(IV) is hexacoordinated with an additional apical methanol ligand *trans* to the oxo. This coordination geometry is known for many vanadyl(IV) complexes,[31] but not reported for vanadyl(IV)porphyrins. The two vanadium-oxygen distances (1.60 Å for V=O and 2.32 Å for the V-O) are in the usual range found for other vanadium(IV) complexes (see Figure 1). This unusual coordination leads to the formation of dimeric assemblies in the solid state held together by hydrogen bonds between the methanol OH and the ketone function of another porphyrin (see Figure 2). These symmetric assemblies are also stabilized by π-π interactions between the extended aromatic parts of these porphyrins (with average distances of 3.5 to 3.6 Å between the aromatic planes).

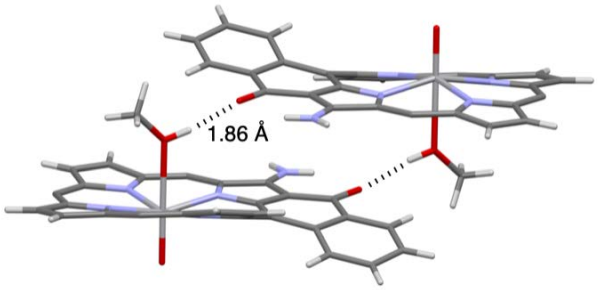

Figure 2. X-ray structure of vanadylporphyrin 5: assembly of two porphyrins in the solid state through intermolecular hydrogen bonds ($d_{O\text{-}H}$ = 1.86 Å) and π-π stacking (*meso*-phenyl groups omitted for clarity).

The enaminoketone functionalities located at the periphery of these vanadylporphyrins were then used to construct porphyrin dimers by complexation of different metal ions. Using palladium(II) (Scheme 2) or platinum(II) (Scheme 3) ions afforded porphyrin dimers linked by these metal ions, that were known to form square planar complexes.

Scheme 2. Preparation of the vanadylporphyrin dimers 7 and 8.

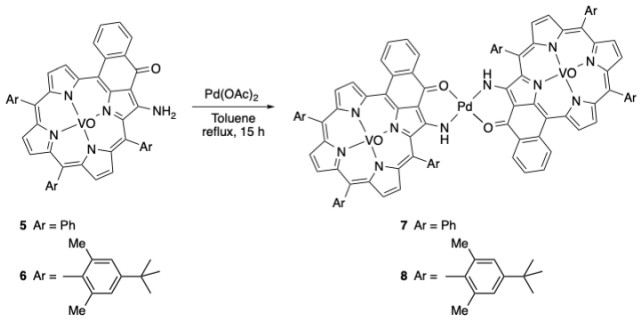

Once again, single crystals suitable for X-ray crystallography were obtained for dimer **7** bearing *meso*-phenyl substituents with palladium(II) as a linking ion. As expected the coordination geometry around of the linking palladium(II) is square planar and *trans*. In this dimer, the vanadyl(IV) coordination geometry is square pyramidal with no additional apical methanol ligand. The two porphyrins are ruffled as expected for these extended porphyrins. Two isomers, called α,α and *α,β*, are possible for these dimers depending on the relative orientations of the oxides relative to the molecular plane. The major product was always the *α,β* isomer possessing a center of symmetry (one vanadyl up and the other down). The distance between the two vanadium(IV) ions is 14.34 Å. A similar structure (isomer *α,β* with very similar distances between the vanadium(IV) ions) was obtained for the *meso*-aryl substituted dimer **8**, but unfortunately with disorders in the solvents included in the unit cell which affected the resolution (see a view of the molecule in the supporting information figure S7).

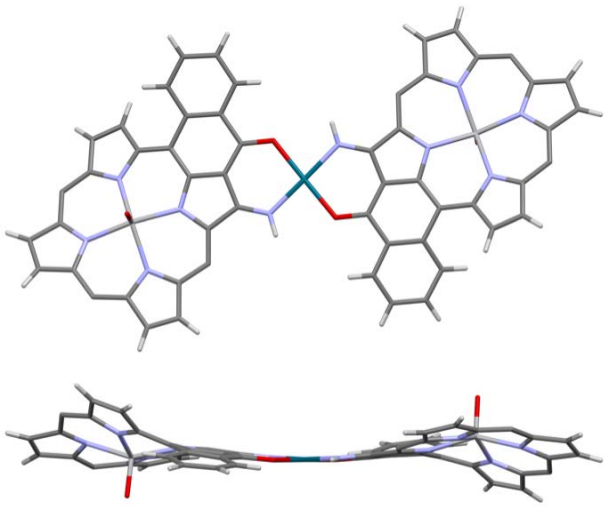

Figure 3. X-ray structure of porphyrin dimer **7**: two orthogonal views (six *meso*-phenyl groups omitted for clarity), showing clearly the isomer was the α–β and that the coordination geometry around the palladium(II) unit was *trans*.

Preparing platinum linked dimers proved to be more difficult. First attempts using traditional synthetic methods were unsuccessful: even prolonged heating of porphyrin **6** and $Pt(acac)_2$ in refluxing dichlorobenzene did not give the expected dimer. By contrast, microwave heating at 200°C (Scheme 3) led to two dimeric compounds that could be separated by chromatography. The centrosymmetric isomer **9** (less polar isomer α–β) was the major product and a second minor isomer (more polar, but with the same mass and a very similar electronic spectrum, thus isomer α–α, see supporting information figures S5 and S6) was also isolated.

Scheme 3. Preparation of vanadylporphyrin dimers 9.

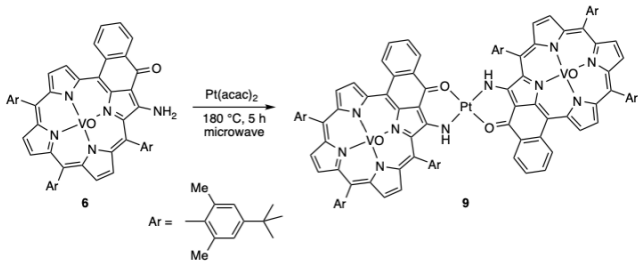

The electronic properties of these dimers were similar to previous results with diamagnetic compounds. Large bathochromic shifts were observed in the electronic spectra of dimers **8** and **9** when compared to monomeric vanadyl(IV) porphyrin **6** (see Figure 4). The Soret bands were much broader in the two dimers and the lowest energy Q-bands shifted from 672 nm (compound **6**) to 718 and 785 nm for dimers **8** and **9**, respectively. As expected and as already observed earlier, replacing a 4d linking metal ion by a 5d metal ion led to a larger bathochromic shift and hence a better electronic delocalization between the two aromatic macrocycles.

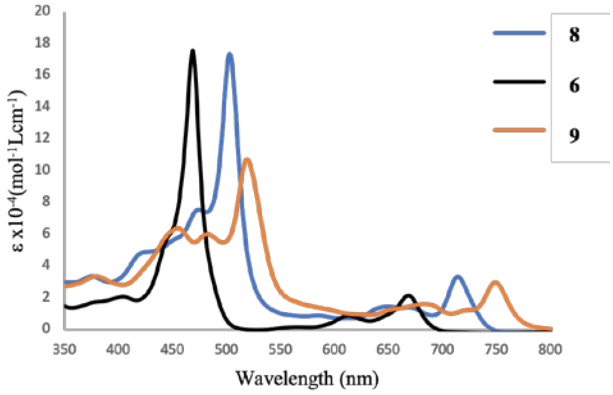

Figure 4. Electronic spectra of vanadyl(IV) porphyrin **6** and porphyrin dimers **8** and **9** (isomer α–β).

Electrochemical measurements led to the same conclusions. It was stated by Therien that the splitting of the first oxidation waves in the cyclic voltammetry (CV) in porphyrin dimers was a good indication of the extent of electronic delocalization.[32] The electrochemistry of vanadyl(IV)porphyrin derivatives is well established.[33] These compounds undergo two oxidation steps leading to a π-radical-cation and a dication and two reduction steps leading to a π-radical-anion and a dianion. Vanadyl(IV)porphyrin **6** underwent as expected two reversible oxidation and reduction steps (see Figure S8). The first oxidation of dimers **8** and **9** took place at lower potentials (see Figure S9) than the oxidation of **6** and the splitting of the first oxidation waves in the CV was present and increased significantly for dimer **9** α–β (see Table 1). For dimers **8** and **9**, after the first oxidation step leading to a π-radical-cation, the radical-cation is delocalized significantly over the entire molecule and consequently the second oxidation occurs at a higher potential. This delocalization varies by changing the linking metal ion and thus the splitting is more pronounced for the 5d platinum(II) compared to the 4d palladium(II) linkage. The splitting was not observed for the reduction as there was no communication between the porphyrin moieties on reduction. This meant that there was no delocalization of the π-radical-anion and hence no splitting was observed. This was corroborated by DFT calculations (B3LYP). The calculations showed that the HOMO was dπ/π-type in character with a metallic contribution from the linking metal ion that led to delocalization over the porphyrin moieties, whereas no metallic contribution was present in the LUMO and no delocalization occured between the two porphyrins during the reduction.

Table 1. Oxidation potentials for compounds 6, 8 and 9.

Compound	E_{ox1} (volts)	E_{ox2} (volts)	E_{ox3} (volts)	E_{ox2} - E_{ox1} (mV)
6	0.559	0.853		
8	0.420	0.584	0.883	164
9 (α–β)	0.455	0.683	0.904	228

Cyclic voltammetry: dichloromethane, 0.1 M NBu_4PF_6 at a scan rate of 0.1 V/s, glassy carbon electrode, volt *vs* Fc^+/Fc as internal reference.

The two isomers of the platinum(II) linked dimers presented almost identical absorption spectra and cyclic voltammetry, consequently only the CV and electronic spectrum of dimer **9**-*α,β* is shown in Table 1 and Figure 4. This was not too surprising as the interactions discussed here are ligand based and it was the linking metal ion that determined the communication between the two sub-units.

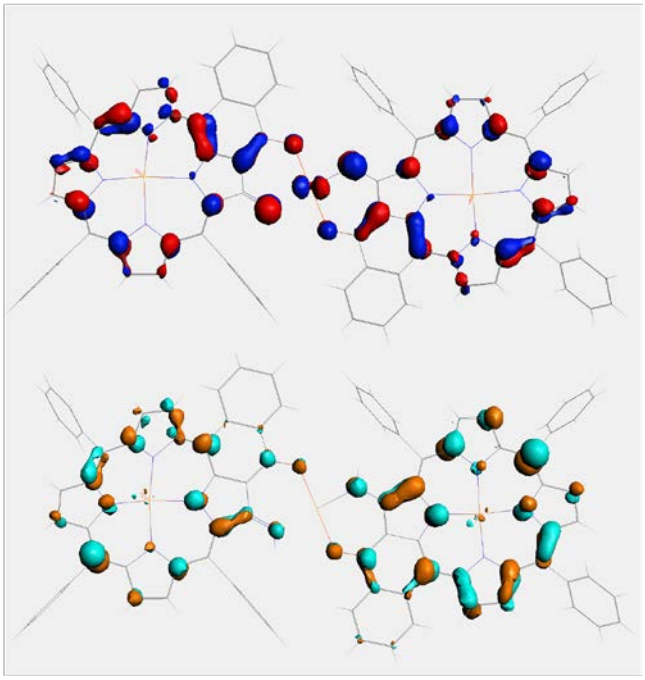

Figure 5. Frontier molecular orbitals of dimer **8**: top HOMO and bottom LUMO (DFT calculations, B3LYP).

The Continuous Wave Electron Paramagnetic Resonance (CW EPR) spectrum of a frozen solution of vanadyl(IV) porphyrin **6** exhibited the typical line shape of vanadyl complexes and was comparable with the EPR spectra of other vanadyl porphyrins described in the literature (see Figure 6).[34]

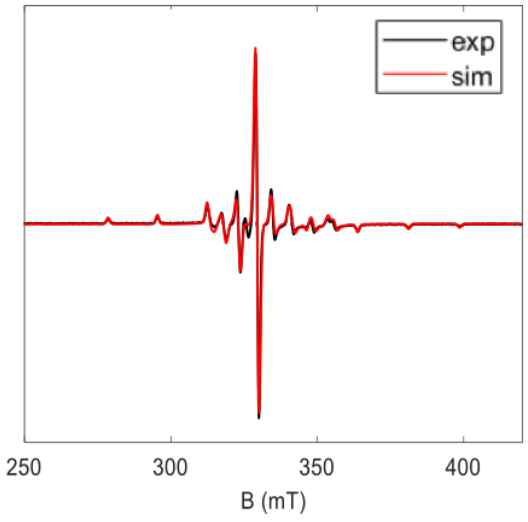

Figure 6. X-band experimental (black line) and simulated (red line) EPR spectra of vanadylporphyrin **6** (10^{-4} M in 80/20 $CH_2Cl_2/CHCl_3$) at 15 K recorded with a microwave power of 0.1 mW and a modulation amplitude of 0.5 mT.

This characteristic features results from the hyperfine interaction of unpaired electron spin $S = 1/2$ of V^{4+} ($3d^1$) with the $I = 7/2$ nuclear spin ^{51}V isotope (99.75% abundant). The planar structure of the porphyrin leads to **g** and **A**-tensors with an approximatively axial symmetry. The *A* values for the main orientations (x, y, and z) were as follows, 170, 152 and 472 MHz.

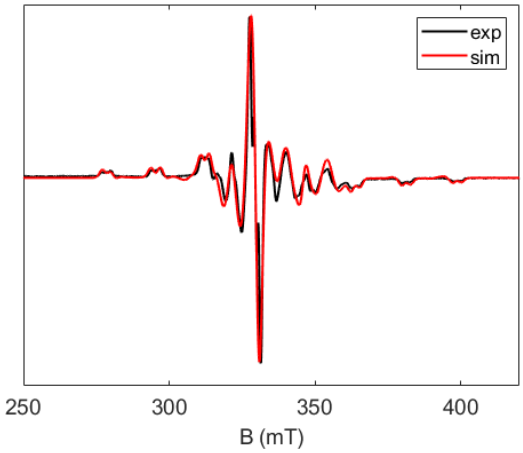

Figure 7. X-band experimental and simulated EPR spectra of porphyrin dimer **8** (10^{-4} M in 80/20 $CH_2Cl_2/CHCl_3$) at 15 K recorded with a microwave power of 0.1 mW and a modulation amplitude of 0.4 mT.

Taking into account the local symmetry at the porphyrin site (**g** and **A** tensors were assumed axial and colinear) the spectrum was simulated very satisfactorily using an axial spin-Hamiltonian with a set of parameters given in Table 2 (*vide infra).* The EPR spectrum of dimer **8** (see Figure 7) was recorded in the same conditions and it appeared to be very similar to that of the vanadyl(IV) porphyrin **6** with one pertinent difference. The two spectra (**6** and **8**) superimpose onto each other with similar *g* factors but a closer comparison showed a small splitting in each peak, indicating the presence of magnetic interactions between the two vanadyl units. This distinguishable interaction was present despite the fact that the two metal sites were quite far apart (14.3 Å found in the crystal structure).

To simulate the EPR spectrum, we added a term to the spin Hamiltonian to account for the electron spin-spin interaction. The singlet ($S = 0$) and triplet ($S = 1$) states arising from the interaction of two VO porphyrin units were separated by the magnitude of the isotropic exchange interaction, whereas the levels within the triplet state were separated by the magnetic dipole-dipole interaction and anisotropic exchange terms that may eventually be operative. Consequently, the triplet and singlet states are mixed, complicating the EPR spectrum. With this assumption, for **8** the major contribution arises mainly from a through-space dipolar interaction (*D*) with only a small effect from exchange terms. The distance, *r*, between the two VO units can be evaluated with the following equation:[35]

$$D = \frac{3\, g\, \mu_B}{2r^3} = 1.39 \times 10^4 \frac{g}{r^3} \qquad \text{(eq.1)}$$

Where μ_B is the Bohr magneton and r is the distance in Å and D in Gauss.

This equation is applied assuming the point-dipole approximation. With a D value of 40 MHz measured from the spectrum, an r value of 13 Å was calculated. This value was close to that obtained by X-ray crystallography. The spectrum was fitted using Easyspin[36] with the following Hamiltonian that encompasses the **g** tensor, hyperfine tensor **A** for both VO porphyrin units and the electron-electron interaction matrix J:

$$\hat{H} = \mu_B \sum_{i=1}^{2} \mathbf{B}\mathbf{g}_i^{V}\hat{\mathbf{S}}_i^{V} + \sum_{i=1}^{2} \hat{\mathbf{S}}_i^{V}\mathbf{A}_i^{V}\hat{\mathbf{I}}_i^{V} + \hat{\mathbf{S}}_1^{V}\mathbf{J}\hat{\mathbf{S}}_2^{V} \quad \text{(eq.2)}$$

The **J** interaction matrix is composed of all exchange and dipolar terms. Each of those can be decomposed to isotropic, antisymmetric and anisotropic components. Due to the perfectly (for **8** and **9**-α,β) or practically (for **9**-α,α) centrosymmetric structures of our complexes, the antisymmetric term can be neglected based on Moriya's rules, thus **J** can be written as a sum of the isotropic and anisotropic terms:

$$\boldsymbol{J} = J_{iso}S_1S_2 + S_1\mathbf{D}_{\boldsymbol{aniso}}S_2 \quad \text{(eq.3)}$$

$\mathbf{D}_{aniso}$ is a symmetric traceless tensor representing the sum of dipolar interactions and of eventual anisotropic exchange terms.

The obtained values for the **g** and **A** tensors for the monomer **6** were kept the same for the simulation of **8** with the through space dipolar interaction extracted from the EPR spectrum. The best simulated EPR spectrum assessed to the magnitude of $|J|$ of around 6 ± 2 MHz which is a weak coupling regime. The distance between the two vanadyls allows for a simplification of the above equation, as the isotropic exchange and the antisymmetric is assumed to be near zero when the two paramagnetic metals are as far apart as 14 Å.

CW EPR was also carried out on the two isomeric forms of dimer **9**, α,α and α,β (Figure 8). These two dimers were separated by column chromatography (the α,α dimer is more polar than the α,β dimer). Despite the two molecules having identical electronic properties, the magnetic properties of these two dimers were different. The coordination geometry being square pyramidal for vanadylporphyrins, the distances between the two vanadium(IV) in the α,α and the α,β isomers are necessarily different. However, the change in distance still remains small, < 0.4 Å, and consequently the dipolar interactions (D) will be basically identical for the α,α and the α,β dimers. Differences between the spectra shown in Figure 8 are hence assumed to be on account of an increase of isotropic exchange, J. As the two vanadyls are in the same direction for the α,α dimer, this would lead to a favorable electronic pathway between the two porphyrin in this dimer and consequently lead to a more pronounced J coupling. The bottom spectrum of Figure 8 is assigned to the α,β dimer on account of its similarity to the spectrum of dimer **8** which was also α,β and also had a mild splitting in all the peaks. This is to be expected as the interaction is dipolar, i.e. through-space, consequently the linking metal ion between the two porphyrins should not have an impact on the interactions. This point helps confirm the hypothesis that a mild dipolar coupling interaction occurs between the two vanadyl sites, in close agreement with the large distances between them. The top spectrum of Figure 8 has a stronger interaction compared to the bottom spectrum, evident by the increase in line broadening compared to the monomer **6** and the bottom spectrum. This spectrum is assigned to the α,α as the results of the EPR simulation for this isomer leads to a similar D but with a more important J value (see Table 2) indicating a better through-bond interaction in this structure and responsible for the spectral broadening observed. This simulation matches with the experimental results.

Table 2. Best fit EPR parameters obtained for the simulation of the spectra of 6, 8, 9 (α,α) and 9 (α,β).

	Monomer **6**	Dimer **8**	Dimer **9** (α,α)	Dimer **9** (α,β)
g_x ($g$strain)	1.9823 (0.0087)	1.9827 (0.017)	1.9827 (0.017)	1.9827 (0.017)
g_y ($g$strain)	1.9845 (0.0087)	1.9838 (0.017)	1.9838 (0.017)	1.9838 (0.017)
g_z ($g$strain)	1.9636 (0.0075)	1.9634 (0.013)	1.9634 (0.013)	1.9634 (0.013)
A_V (MHz)	170, 152, 472	170, 152, 472	170, 152, 472	170, 152, 472
$\|J\|$ (MHz)		< 6	35	< 6
D (MHz)		42	42	42

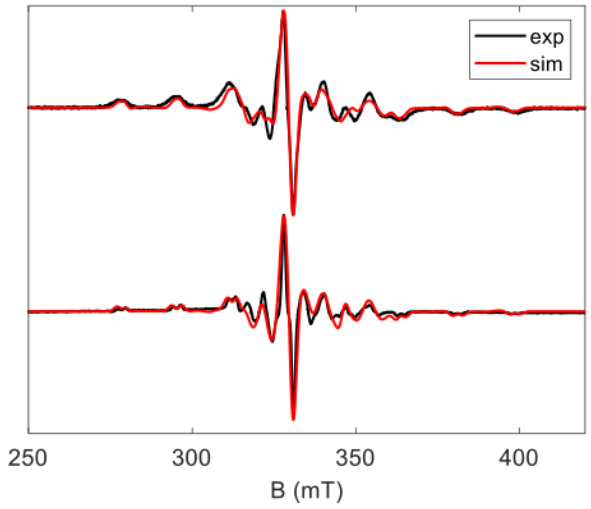

Figure 8: X-band experimental (black) and simulated (red) EPR spectra of the two isomeric forms (α,α (top) and the α,β (bottom)) of dimer **9** (10^{-4} M; 80:20; CH_2Cl_2:$CHCl_3$) recorded at 15 K with a microwave power of 0.1 mW and a modulation amplitude of 0.4 mT.

CONCLUSION

These results demonstrate that the vanadyl(IV) porphyrin platform is ideal for engineering controlled interactions in candidates for the implementation two-qubit (or two-qudit) gates. These molecules are highly stable and their planar structures make them ideal candidates for surface deposition. Moreover, their modular nature suggests the possibility of engineering g-anisotropy by varying one of the two spin centers. This latter is a key requirement for the selective addressing of qubits in two-qubit gates.

EXPERIMENTAL SECTION

General information. Most of the experiments were carried out in standard glassware under inert argon atmosphere. Dichloromethane was distilled from calcium hydride and toluene from sodium/benzophenone ketyl. Chromatographic separations were performed using silica gel (Merck 40-63 μm). ^{1}H and ^{13}C NMR (for the starting compounds) were recorded on a Bruker Avance 500 equipped with a cryoprobe. UV-Visible spectra were obtained on a CARY 5000 UV/vis/NIR double-beam spectrometer in dichloromethane. Elemental analyses were performed by the "Service d'Analyses de la FR 2010 in Strasbourg". X-ray data were collected on a Bruker Photon III diffractometer. X-band continuous wave EPR spectra were recorded on an EMXplus spectrometer (Bruker Biospin GmbH), equipped with a high sensitivity resonator (4119HSW) and an ESR900 continuous flow cryostat controlled with an Oxford ITC503S apparatus (Oxford Instrument). Samples were introduced into 4 mm outer diameter clear fused quartz tubes (Wilmad-LabGlass). Modulation frequency and amplitude were respectively of 100 kHz and 0.4 mT. The *g* factor was calibrated using the Bruker strong pitch ($g = 2.0028$). Starting ketoporphyrin free bases **1** and **2** were prepared according to previously published procedures.[29]

DFT Calculations. The calculations were performed with the ADF 2019 package at DFT level of theory using the B3LYP functional.[37] Scalar relativistic effects were included using zero order regular approximated (ZORA) Hamiltonian.[38] All atoms were described by the TZP basis set. Solvent corrections (dichloromethane) were introduced through a PCM (Polarizable Continuum Model). Van der Waals forces were described through Grimme's corrections.[39]

Vanadyl(IV)porphyrin 3. A solution of base **1** (174 mg, 0.271 mmol), vanadyl(IV) sulfate (163 mg, 0.644 mmol) and sodium acetate (840 mg, 0.1 mol) in acetic acid (27 mL) was refluxed for 20 h. To the resulting solution was added water and dichloromethane. After separation of the organic and the aqueous layer, evaporation of the solvents, crystallization from dichloromethane and methanol, green crystals of **3** (179 mg, 0.254 mmol, 94%) were isolated and used for the next step without further purification.

Vanadyl(IV)porphyrin 4. Vanadyl sulfate (162 mg, 0.640 mmol) and the free-base porphyrin **2** (155 mg, 0.207 mmol) were heated to reflux in an acetic acid buffer (glacial acetic acid (27 mL) and sodium acetate (828 mg) for 20h. Water (50 mL) was then added and the precipitate was filtered and washed with water in order to extract the vanadyl salts (washed until filtrate no longer blue). This afforded the titled product as a green solid (175mg, 0.183 mmol, 88%). Only one spot was present on the TLC plate. MS MALDI-TOF Calcd for $C_{63}H_{62}N_4O_2V$ ($M + H^+$) 958.44; Obsd 958.398.

Vanadyl(IV)porphyrin 5. A solution of vanadyl(IV) porphyrin **3** (170 mg, 0.241 mmol), 4-amino-4H-1,2,4-triazole (253 mg, 3.01 mmol) and sodium hydroxide (1.05 g, 16.0 mmol) in toluene (90 mL) and ethanol (10 mL) was heated to reflux for 2 hours. The resulting green solution was washed three times with water and the organic phase was evaporated. After purification by column chromatography (SiO_2, 9:1 dichloromethane : cyclohexane) the pure vanadyl porphyrin **5** was crystallized in dichloromethane and methanol, and then dried under vacuum. UV-visible (CH_2Cl_2): λ_{max} = 405 (ε = 25 400), 462 (183 000), 611(11 600), 666 (24 100) nm. Elem. Anal. Calcd (%) for $C_{45}H_{27}N_5O_2V.2H_2O$: C, 71.43; H, 4.13; N, 9.26. Found: C, 71.67; H, 3.75; N: 9.17. Single crystals were grown by slow vapor diffusion of methanol in a chloroform solution of **5**. Crystal data $C_{48}H_{33}Cl_6N_5O_3V$: M = 991.43 g.mol^{-1}, monoclinic, space group P 21/n, *a* = 11.4999(4) Å, *b* = 21.6133(7) Å, *c* = 18.0899(6) Å, α = 90°, β = 107.1730(10) °, γ = 90°, V = 4295.8(2) Å^3, Z = 4, ρ_{calc} = 1.533 Mg/m^3, T = 120(2) K, MoK_α = 0.71073 Å, 1.884 < θ < 28.053, 123679 reflections measured, 10406 unique reflections, R_1 = 0.0540, wR_2 = 0.1392, GoF = 1.034. CCDC Nr : 2216948.

Vanadyl(IV)porphyrin 6. Vanadyl(IV) porphyrin **4** (322 mg, 0.34 mmol), 4-amino-4H-1,2,4-triazole (565 mg, 6.72 mmol) and NaOH (1.4 g, 34 mmol) were refluxed for 2 h in a toluene:ethanol (8:2) solution under argon. Water (50 mL) was then added and the organic phase was washed with water and dried over sodium sulphate. The solvent was evaporated and the porphyrin was purified by column chromatography (SiO_2; dichloromethane:cyclohexane 2:1) to afford the titled product (310 mg, 0.32 mmol, 94%). UV-visible (CH_2Cl_2): λ_{max} = 470 (ε = 173 000), 616 (10000), 672 (20000) nm. MS MALDI-TOF: Calcd for $C_{63}H_{63}N_5O_2V$ ($M + H^+$) 973.45; Obsd 973.517.

Vanadyl(IV)porphyrin dimer 7. A solution of **5** (60 mg, 0.083 mmol) and palladium(II) acetate (10 mg, 0.046 mmol) in toluene (25 mL) was refluxed for 15 hours. TLC showed the presence of three products which were separated by column chromatography (SiO_2, 6:4 cyclohexane : dichloromethane). The major product **7** isolated in 47% yield was a vanadyl(IV)porphyrin dimer linked by palladium(II). Two more polar minor products were isolated, most probably structural isomers, because their electronic spectra were similar to the one of **7**. The nature of the major isomer was determined by X-ray crystallography. Single crystals were grown by slow vapor diffusion of methanol in a chloroform solution of **7**. MS-MALDI: Calc. for $C_{90}H_{52}N_{10}O_4PdV_2$ 1544.208 found 1544.195. UV-visible: λ_{max} = 474 (rel. Int. = 0.42), 503 (1), 649 (0.099), 671 (0.096), 713 (0.23). Crystal data $C_{93}H_{55}Cl_9N_{10}O_4PdV_2$: M = 1903.80 g.mol^{-1}, orthorhombic, space group P 21 21 21, *a* = 38.6581(18) Å, *b* = 13.7285(6) Å, *c* = 15.4266(7) Å, α = 90°, β = 90°, γ = 90°, V = 8187.2(6) Å^3, Z = 4, ρ_{calc} = 1.545 Mg/m^3, T = 120(2) K, MoK_α = 1.54178 Å, 2.286 < θ < 66.443, 94102 reflections measured, 14408 unique reflections, R_1 = 0.0686, wR_2 = 0.1724, GoF = 1.090. CCDC Nr: 2216945.

Vanadyl(IV)porphyrin dimer 8. Vanadyl(IV) porphyrin **6** (25 mg, 0.026 mmol) and $Pd(OAc)_2$ (3 mg, 0.14 mmol) were heated to reflux in toluene (10 mL) for 16 h under argon. On cooling the solvent was evaporated and the product was purified by column chromatography (SiO_2; cyclohexane:dichloromethane 60:40) to afford the titled product as a brown solid (11 mg, 5.36 μmol, 42%). UV-visible (CH_2Cl_2): λ_{max} = 476 (ε = 75000), 505 (169 000), 648 (15000), 718 (31000) nm. MS MALDI-TOF: Calcd for $C_{126}H_{124}N_{10}O_4PdV_2$ (M^{o+}) 2048.77; Obsd 2048.573. An X-ray structure was obtained, but not suitable for publication (see supporting information Figure S7). Yet it was apparent that the dimer was the *α-β* isomer.

Vanadyl(IV)porphyrin dimers 9. Vanadyl(IV) porphyrin **6** (20 mg, 0.02 mmol) and $Pt(acac)_2$ (4.4 mg, 0.011 mmol) were heated in 1,2-dichlorobenzene (5 mL) in a microwave (180 °C, 200 mW) for 5 h. On cooling the solvent was evaporated by trap to trap distillation and the product was purified by column chromatography (SiO_2; cyclohexane:dichloromethane 60:40) to afford the titled product in two forms *α,β* (2 mg, 0.93 μmol, 10%) and *α,α* (5 mg, 2 μmol, 20%) both as brown solids. UV-visible (CH_2Cl_2): λ_{max} = 452 (ε = 63000), 485 (60000), 518 (110000), 688 (16000), 753 (30000) nm. MS MALDI-TOF: Calcd for *α,β*: $C_{126}H_{124}N_{10}O_4PtV_2$ ($M + H^+$) 2138.84; obsd 2138.773. MS MALDI-TOF: Calcd for *α,α* $C_{126}H_{124}N_{10}O_4PtV_2$ ($M + H^+$) 2138.84; obsd 2138.858.

ASSOCIATED CONTENT

Supporting Information

The Supporting Information is available free of charge on the ACS Publications website.

Mass spectra of vanadyl(IV) porphyrin monomers and dimers (PDF) and cyclic voltammetry of compounds **6** and **8**. Ciffiles of compounds **5** and **7**.

AUTHOR INFORMATION

Corresponding Author

* Romain Ruppert - Institut de Chimie, UMR CNRS 7177, Universite de Strasbourg, 4 rue Blaise Pascal, 67000 Strasbourg (France)
0000-0002-1513-1949 Email: rruppert@unistra.fr

Authors

Jordan L. Appleton - Institut de Chimie, UMR CNRS 7177, Universite de Strasbourg, 4 rue Blaise Pascal, 67000 Strasbourg (France)
0000-0002-8844-6466

Nolwenn Le Breton - Institut de Chimie, UMR CNRS 7177, Universite de Strasbourg, 4 rue Blaise Pascal, 67000 Strasbourg (France)
0000-0002-5638-9444

Mary-Ambre Carvalho - Institut de Chimie, UMR CNRS 7177, Universite de Strasbourg, 4 rue Blaise Pascal, 67000 Strasbourg (France)
0000-0002-3454-0086

Jean Weiss - Institut de Chimie, UMR CNRS 7177, Universite de Strasbourg, 4 rue Blaise Pascal, 67000 Strasbourg (France)
0000-0001-7753-8958

Athanassios K. Boudalis - Institut de Chimie, UMR CNRS 7177, Universite de Strasbourg, 4 rue Blaise Pascal, 67000 Strasbourg (France)
0000-0002-8797-1170

Christophe Gourlaouen - Institut de Chimie, UMR CNRS 7177, Universite de Strasbourg, 4 rue Blaise Pascal, 67000 Strasbourg (France)
0000-0002-2409-2849

Sylvie Choua - Institut de Chimie, UMR CNRS 7177, Universite de Strasbourg, 4 rue Blaise Pascal, 67000 Strasbourg (France)
0000-0003-1005-3555

Author Contributions

The manuscript was written through contributions of all authors. All authors have given approval to the final version of the manuscript.

Funding Sources

Any funds used to support the research of the manuscript should be placed here (per journal style).

ACKNOWLEDGMENTS

The authors gratefully acknowledge the University of Strasbourg and the CNRS for continuous financial support. J.L.A. thanks the French Ministry of Research for his PhD fellowship. M.A.C. thanks the FRC-Labex CSC for her fellowship (ANR-10-LABX-0026 CSC).

REFERENCES

(1) Kahn, O. In "Molecular Magnetism", VCH, New York, **1993**.

(2) Coronado, E. Molecular magnetism: from chemical design to spin control in molecules, materials and devices. *Nat. Rev. Mater.* **2020**, *5*, 87-104.

(3) Zadrozny, J. M.; Niklas, J.; Poluektov, O. G.; Freedman, D. E. Multiple quantum coherences from hyperfine transitions in a vanadium(IV) complex. *J. Am. Chem. Soc.* **2014**, *136*, 15841-15844.

(4) Zadrozny, J. M.; Niklas, J.; Poluektov, O. G.; Freedman, D. E. millisecond coherence time in a tunable molecular electronic spin qubit. *ACS Cent. Sci.* **2015**, *1*, 488-492.

(5) Graham, M. J.; Krzyaniak, M.; Wasielewski, M. R.; Freedman, D. E. Probing nuclear spin effects on electronic coherence via EPR measurements of vanadium(IV) complexes. *Inorg. Chem.* **2017**, *56*, 8106-8113.

(6) Graham, M. J.; Yu, C.-J.; Krzyaniak, M.; Wasielewski, M. R.; Freedman, D. E. Synthetic approach to determine the effect of nuclear spin distance on electronic spin decoherence. *J. Am. Chem. Soc.* **2017**, *139*, 3196-3201.

(7) Jain, S. K.; Yu, C.-J.; Wilson, C. B.; Tabassum, T.; Freedman, D. E.; Han, S. dynamic nuclear polarization with vanadium(IV) metal centers. *Chem.* **2021**, *7*, 421-435.

(8) Atzori, M.; Morra, E.; Tesi, L.; Albino, A.; Chiesa, M.; Sorace, L.; Sessoli, R. Quantum coherence times enhancement in vanadium(IV)-based potential molecular qubits: the key role of the vanadyl moiety. *J. Am. Chem. Soc.* **2016**, *138*, 11234-11244.

(9) Yamabayashi, T.; Atzori, M.; Tesi, L.; Cosquer, G.; Santanni, F.; Boulon, M.-E.; Morra, E.; Benci, S.; Torre, R.; Chiesa, M.; Sorace, L.; Sessoli, R.; Yamashita, M. Scaling up electronic spin qubits into a three-dimensional metal-organic framework. *J. Am. Chem. Soc.* **2017**, *139*, 3196-3201.

(10) Tesi, L.; Lucaccini, E.; Cimatti, L.; Perfetti, M.; Mannini, M.; Atzori, M.; Morra, E.; Chiesa, M.; Caneschi, A.; Sorace, L.; Sessoli, R. Quantum coherence in a processable vanadyl complex: new tools for the search of molecular spin qubits. *Chem. Sci.* **2016**, *7*, 2074-2083.

(11) Yu, C.-J.; Graham, M. J.; Zadrozny, J. M.; Niklas, J.; Krzyaniak, M.; Wasielewski, M. R.; Poluektov, O. G.; Freedman, D. E.Long coherence times in nuclear spin-free vanadyl qubits. *J. Am. Chem. Soc.* **2016**, *138*, 14678-14685.

(12) Moreno-Pineda, E.; Godfrin, C.; Balestro, F.; Wernsdorfer, W.; Ruben, M. Molecular spin qubits for quantum algorithms. *Chem. Soc. Rev.* **2018**, *47*, 501-513.

(13) Gimeno, L.; Urtizberea, A.; Roman-Roche, J.; Zueco, D.; Camon, A.; Alonso, P. J.; Roubeau, O.; Luis, F. Broad-band spectroscopy of a vanadyl porphyrin: a model electronuclear spin qubit. *Chem. Sci.* **2021**, *12*, 5621-5630. Chicco, S.; Chiesa, A.; Allodi, G.; Garlatti, E.; Atzori, M.; Sorace, L.; De Renzi, R.; Sessoli R.; Carretta S. Controlled coherent dynamics of [VO(TPP)], a prototype molecular nuclear qudit with an electronic ancilla, *Chem. Sci.* **2021**, *12*, 12046-12055. Atzori M.; Garlatti, E.; Allodi, G.; Chicco, S.; Chiesa, A.; Albino, A.; De Renzi, R.; Salvadori, E.; Chiesa, M.: Carretta, S.; Sorace, L. Radiofrequency to Microwave Coherent Manipulation of an Organometallic Electronic Spin Qubit Coupled to a Nuclear Qudit. *Inorg. Chem.* **2021**, *60*, 15, 11273–11286.

(14) Callot, H. J.; Ocampo, R. Geochemistry of porphyrins in "The Porphyrin Handbook", Kadish, K. M.; Smith, K. M.; Guilard, R. Eds, Academic Press, San Diego, **2000**, Vol 1, Ch. 7, 349-398.

(15) Leznoff, C. C.; Lam, H.; Marcussio, S. M.; Nevin, W. A.; Janda, P.; Kobayashi, N.; Lever, A. B. P. A planar binuclear phthalocyanine and its dicobalt derivatives. *J. Chem. Soc., Chem. Commun.* **1987**, 699-701.

(16) Lelièvre, D.; Bosio, L.; Simon, J.; André, J.-J.; Bensebaa, F. Dimeric substituted copper phthalocyanine liquid crystals. Synthesis, characterization and magnetic properties. *J. Am. Chem. Soc.* **1992**, *112*, 4475-4479.

(17) Zhao, M.; Stern, C.; Barrett, A. G. M.; Hoffman, B. M. Porphyrazines as molecular scaffolds: periphery-core spin coupling between metal ions of a Schiff base porphyrazine. *Angew. Chem. Int. Ed.* **2003**, *42*, 462-465.

(18) Matano, Y.; Fujii, D.; Shibano, T.; Furukawa, K.; Higashino, T.; Nakano, H.; Imahori, H. Covalently linked 5,15-diazaporphyrin dimers:

promising scaffolds for a highly conjugated azaporphyrin π system. *Chem. Eur. J.* **2014**, *20*, 3342-3349.

(19) Kobayashi, N.; Numao, N.; Kondo, R.; Nakajima, S.; Osa, T. A planar binuclear terabenzoporphyrin and its dicopper derivative. *Inorg. Chem.* **1991**, *30*, 2241-2244.

(20) Chmielewski, P. J. Lucky seven: characterization of stable T-shaped copper(II) complexes of [32]heptaphyrins. *Angew. Chem. Int. Ed.* **2010**, *49*, 1359-1361.

(21) Toganoh, M.; Furuta, H. Blooming of confused porphyrinoids-fusion, expansion, contraction and more confusion. *Chem. Commun.* **2012**, 937-954.

(22) Ikeue, T.; Furukawa, K.; Hata, H.; Aratani, N.; Shinokubo, H.; Kato, T.; Osuka, A. The importance of a β–β bond for long-range antiferromagnetic coupling in directly linked copper(II) and silver(II) diporphyrins. *Angew. Chem. Int. Ed.* **2005**, *44*, 6899-6901.

(23) Pozo, I.; Lombardi, F.; Alexandropoulos, D. I.; Kong, F.; Deng, J.-R; Horton, P. N.; Coles, S. J.; Myers, W. K.; Bogani, L.; Anderson, H. L. Conjugated porphyrin tapes as quantum mediators for vanadyl qubits. *ChemRxiv, Inorg. Chem.* **2022**. DOI: 10.26434/chemrxiv-2022-1v5b4.

(24) Richeter, S.; Jeandon, C.; Gisselbrecht, J.-P.; Ruppert, R.; Callot, H. J. Syntheses and optical and electrochemical properties of porphyrin dimers linked by metal ions. *J. Am. Chem. Soc.,* **2022**, *124*, 6168-6179.

(25) Richeter, S.; Jeandon, C.; Ruppert, R.; Callot, H. J. A modular approach to porphyrin oligomers using metal ions as connectors. *Chem. Commun.* **2002**, 266-267.

(26) Carvalho, M.-A.; Dekkiche, H.; Karmazin, L.; Sanchez, F.; Vincent, B.; Kanesato, M.; Kikkawa, Y.; Ruppert, R. Synthesis and study at a solid/liquid interface of porphyrin dimers linked by metal ions. *Inorg. Chem.* **2017**, *56*, 15081-15090.

(27) Carvalho, M.-A.; Dekkiche, H.; Nagasaki, M.; Kikkawa, Y.; Ruppert, R. Coordination-driven construction of porphyrin nanoribbons at a highly oriented pyrolytic graphite (HOPG)/liquid interface. *J. Am. Chem. Soc.* **2019**, *141*, 10137-10141.

(28) Carvalho, M.-A.; Dekkiche, H.; Richeter, S.; Bailly, C.; Karmazin, L.; McKearney, D.; Leznoff, D. B.; Rogez, G.; Vileno, B.; Choua, S.; Ruppert, R. Antiferromagnetic coupling in copper(II)porphyrin dimers linked by copper(II) or palladium(II) ion. *J. Porphyrins Phthalocyanines*, **2020**, *24*, 238-246.

(29) Dekkiche, H.; Carvalho, M.-A.; Jeandon, C.; Karmazin, L.; Boudon, C.; Ruhlmann, L.; Ruppert, R. Synthesis and electrochemistry of nickel(II)porphyrins bearing external palladium(II) or platinum(II) complexes. *J. Porphyrins Phthalocyanines*, **2021**, *25*, 1133-1142.

(30) Erdman, J. G.; Ramsay, V. G.; Kalenda, N. W.; Hanson, W. E. Synthesis and properties of porphyrin vanadium complexes. *J. Am. Chem. Soc.*, **1956**, *78*, 5844-5847. Buchler J. W. in *Porphyrins and Metalloporphyrins*, Ch. 5, Smith, K. M. Ed., 1975, Elsevier.

(31) See for example: Tasiopoulos, A. J.; Troganis, A. N. ; Evangelou, A.; Raptopoulou, C. P.; Terzis, A. Deligiannakis Y.; Kabanos, T. A.; Synthetic Analogues for Oxovanadium(IV)–Glutathione Interaction: An EPR, Synthetic and Structural Study of Oxovanadium(IV) Compounds with Sulfhydryl-Containing Pseudopeptides and Dipeptides. Chem. Eur. J., 1999, 5, 910–921.

(32) Lin, V. S. Y.; DiMagno, S.G.; Therien, M. J. Highly conjugated, acetylenyl bridged porphyrins: new models for light harvesting antenna systems. *Science*, **1994**, *264*, 1105-1111.

(33) Kadish, K. M.; Van Caemelbecke, E.; Royal G. in *The Porphyrin Handbook*, Academic Press San Diego, **2000**, Kadish, K. M.; Smith, K. M.; Guilard, R. Eds, Vol. 8, 1-114.

(34) Espinosa, M. P.; Campero, A.; Salcedo, R. Electron spin resonance and electronic structure of vanadyl-porphyrin in heavy crude oils. *Inorg. Chem.* **2001**, *40*, 4543-4549.

(35) Eaton, S.S.; Eaton, G. R. *Biomed. EPR*, Part B Methodol. Instrumentation Dyn., **2005**, Ch. 8, 223-236.

(36) Stoll, S.; Schweiger, A. Easy spin, a comprehensive software package for spectral simulation and analysis in EPR. *J. Magn. Reson.* **2006**, *178*, 42-55.

(37) Becke, A.D. Density-functional thermochemistry. III. The role of exact exchange. *J. Chem. Phys.* **1993**, *98*, 5648-5652

(38) ADF, SCM, Theoretical Chemistry, Vrije Universiteit, Amsterdam, The Netherlands. Available online: https://www.scm.com/doc/ADF/index.html (accessed on 1 June 2019).

(39) Grimme, S.; Antony, J.; Ehrlich, S.; Krieg, H. A consistent and accurate ab initio parametrization of density functional dispersion correction (DFT-D) for the 94 elements H-Pu. *J. Chem. Phys.* **2010**, *132*, 154104.